CDF note 8212

Measurement of the J/ψ Spin Alignment in $\overline{\mathrm{p}}\mathrm{p}$ Collisions at $\sqrt{s} = 1.96$ TeV

The CDF Collaboration
URL http://www-cdf.fnal.gov
(Dated: July 16, 2006)

We have measured the spin alignment of J/ψ mesons having $5 \leq p_T < 30$ GeV/c and rapidity $|\mathrm{y}| < 0.6$, using the J/$\psi \to \mu^+\mu^-$ decay channel. The analysis is performed using data from $\overline{\mathrm{p}}\mathrm{p}$ collisions at 1.96 TeV with an integrated luminosity of 800 pb^{-1} taken from June 2004 to February 2006 with the CDF II detector at the Fermilab Tevatron. Promptly-produced J/ψ mesons are isolated from those produced in heavy flavor decays by impact parameter selections on the two muon tracks. The analysis procedure is similar to that used in Run I, employing a template method to account for acceptance and trigger efficiency effects. We use experimentally-derived trigger efficiency functions to produce the templates. We measure the polarization $\alpha_B = -0.066 \pm 0.050$ for the B-decay events. We find negative (longitudinal) polarization in the higher p_T region for the prompt J/ψ events, in contrast to expectations from NRQCD.

Preliminary Results for Summer 2006 Conferences

I. INTRODUCTION

A. Prompt J/ψ Production Mechanisms

The production mechanism for J/ψ mesons in high energy $\overline{\rm p}$p collisions is not well understood. Prior to the first measurement of the production cross section at the Tevatron during Run I [1], production was expected to occur via the color-singlet mechanism (CSM), in which gluon-gluon fusion produces a color-octet $c\overline{c}$ pair, followed by real gluon emission to carry away the color and leave a colorless quarkonium state. This leading-order (LO) QCD picture predicted that the ground state J/ψ production cross section would suppressed by the small QCD coupling and by the additional phase space factor associated with the gluon emission compared to production of the p-wave χ_c states. Therefore, most J/ψ events in the CSM were expected to come from decays of χ_c mesons. The Tevatron Run I measurements showed that at most 30% of prompt J/ψ production came from χ_c states [2]. The CSM calculation underestimated the direct production cross section by an order of magnitude for the J/ψ mesons and nearly a factor of 50 for the $\psi(2S)$ mesons.

To address the discrepancy, the color-octet mechanism (COM) [3] was introduced. In this picture the $c\overline{c}$ pair produced in a color-octet state became a color-singlet quarkonium state by interacting with soft gluons. There were no constraints on the initial color or angular momentum quantum numbers of the $c\overline{c}$ pair. The model had adjustable hadronization parameters that allowed it to match the observed p_T-dependence and amplitude of production. Later the model was developed into non-relativistic QCD (NRQCD), attributing the hadronization parameter to be non-perturbative effects that could be factorized from the initial hard scatter. These non-perturbative effects are assumed to be universal and are adjusted to give the best fit to experimental data. The model is expected to break down at small values of the quarkonium transverse momentum. Therefore predictions for the total quarkonium cross section in the NRQCD approach must be treated with caution. A consequence of the model is that the J/ψ mesons would be produced with transverse polarization, especially at large p_T, due to the contribution of large-p_T gluons. The Run I data did not show such an effect, but the amount of data in the p_T range above 15 GeV/c, where the model expected to work well, were not sufficient enough to make a definite conclusion [4–6].

Recently a different approach to the hadronization problem has been introduced, based on Pomeron ideas [7]. In this model gluon-gluon scattering produces the J/ψ meson along with another gluon that is absorbed by a nearby parton in a NNLO process. The sum over many nearby partons boosts the cross section for this process to a dominant level. The model contains parameters that are adjusted to fit the observed prompt cross section and predicts that the prompt production will dominate over feed-down from χ_c states, as had been measured. It also releases the transverse polarization constraint on prompt J/ψ at large p_T. Indeed, the prediction in Ref. [7] is that the J/ψ polarization will be longitudinal for $p_T > 15$ GeV/c.

B. J/ψ Spin Alignment and Decay Angular Distributions

In the rest frame of the J/ψ meson, the μ^+ makes an angle θ^* with respect to the J/ψ direction in the lab frame. The angular distribution depends on the polarization parameter α, which lies in the interval -1 to 1:

$$\frac{d\,\Gamma}{d\cos\theta^*} \propto 1+\alpha\cos^2\theta^*. \tag{1}$$

If the J/ψ meson is fully polarized in the transverse direction, $\alpha = 1$. If it is fully aligned longitudinally, $\alpha = -1$. In our later discussion we use a related alignment parameter η that measures the fraction of longitudinal alignment. The two parameters are simply related:

$$\eta = \frac{1-\alpha}{3+\alpha} \quad (0 \le \eta \le 1). \tag{2}$$

C. Motivation

The Collider Detector at Fermilab (CDF) Collaboration previously reported results on the production of J/ψ mesons using early Run II data [8], confirming the large production cross section and providing a measurement of the $p_T(\mathrm{J}/\psi)$ production spectrum. In this Letter, we re-evaluate the Run I polarization measurements as a prelude to extending the p_T range of the measurement well beyond the Run I limit of 20 GeV/c. The CDF II detector has a large dimuon acceptance and systematic effects in the polarization measurement should be low if the detector response is uniform. The Run II J/ψ trigger was designed to be efficient over a wide p_T range and to provide a large-statistics sample. The data used for this measurement were taken subsequent to the data published in [8], using the same trigger.

II. DETECTOR DESCRIPTION

CDF II is a general purpose detector designed to study high energy $\bar{p}p$ collisions at $\sqrt{s} = 1.96$ TeV. Its components pertinent to this analysis are described briefly below. A more complete description can be found elsewhere [9].

CDF II has a cylindrical symmetry about the beam line, making it convenient to use a cylindrical coordinate system with the z axis along the proton beam direction. We define r to be the distance from the beam line and ϕ to be the azimuthal angle around the beam line. The polar angle θ is measured with respect to the positive z axis and the pseudorapidity η is defined as $-\ln\left[\tan(\theta/2)\right]$. The transverse momentum of a particle is denoted as $p_T = p\sin\theta$.

A silicon vertex detector (SVX II), located immediately outside the beam pipe, provides a precise three-dimensional track reconstruction and is used to identify displaced vertices associated with heavy flavor decays. The momentum of charged particles is measured in the central outer tracker (COT), a multiwire drift chamber that is immersed in a 1.4 T superconducting solenoidal magnet. Outside the COT are electromagnetic and hadronic calorimeters arranged in a projective-tower geometry, covering the $|\eta| < 3.5$. Drift chambers outside the calorimeter identify muon candidates. The central muon (CMU) and central muon upgrade (CMP) detectors cover $|\eta| < 0.6$. The CMP is arranged in a rectangular array around the CMU behind an additional steel shielding to provide further discrimination between real muons and hadronic punch through. Another set of chambers, the central muon extension (CMX), covers $0.6 < |\eta| < 1.0$. This analysis consider only muons in the CMU/P fiducial region.

III. DATA SAMPLE & EVENT SELECTION

This analysis is based on an integrated luminosity of 786 ± 46 pb^{-1} [11, 12] collected with the CDF II detector between June 2004 and February 2006. Events containing J/ψ decays are collected using central dimuon triggers in the CDF three-level trigger system. The first two levels, named Level-1 (L1) and Level-2 (L2), are implemented in hardware. At L1, the COT track is extrapolated to the muon chambers and is required to match a muon track segment. Misalignment and multiple scattering effects are considered in this projection. At L2, silicon hits from the SVX II are added to candidate tracks, if available. A COT-SVX II track is formed only if at least three $r-\phi$ hits in the SVX II are associated with the COT track. The third level, Level-3 (L3), consists of software algorithms that run a stream-lined version of the full CDF reconstruction software. At L3, a full three-dimensional track fit defines the track parameters and a muon stub finding algorithm refines the muon matching requirements. The central dimuon triggers select events having two muon candidates with $p_T > 1.5$ GeV/c at L1. At L2, opening angle and opposite-charge cuts are imposed on a muon pair. At L3, these two opposite-sign muon tracks are required to be within 5 cm in z and to have an invariant mass from 2.7 to 4.0 GeV/c^2.

Additional offline requirements are placed on the muon pairs having an invariant mass between 2.7 and 3.5 GeV/c^2 for the polarization measurement. The invariant mass of the muon pair is calculated constraining the two muons to come from a common vertex. The primary vertex of the event is approximated by the run-averaged beam position (x, y) calculated from silicon tracks and z position calculated from the dimuon vertex fit. For J/ψ candidates, the fit must converge with a Prob $(\chi^2) \geq 0.001$ and $\sigma_{L_{xy}} \leq 0.025$ cm, where a signed two-dimensional decay length L_{xy} is defined as a displacement of the J/ψ vertex projected onto the direction of the $p_T(J/\psi)$. Both muon tracks are required to have $p_T > 1.75$ GeV/c to minimize biases due to trigger thresholds. The transverse momentum of J/ψ candidates must be at least 5 GeV/c in order to maintain reasonable acceptance, given the 1.75 GeV/c muon p_T thresuold. The opening angle $\Delta\phi$ between two muons is required to be less than 2.25 radians. The z position of each muon track is required to be within 60 cm from the center of the detector. We require each muon track to be a COT-SVX II track in order to assure a good lifetime and impact parameter measurement. We also require that each J/ψ candidate has rapidity $|y| < 0.6$.

After all of the requirements above, the data contain 1,014,200 J/ψ candidates within the mass window of $(M_{J/\psi} - 3\sigma,\ M_{J/\psi} + 3\sigma)$, where $M_{J/\psi}$ is the fitted mass of dimuon system and σ is the dimuon mass fit resolution, above a background of 89,200 events. The background is estimated from two sideband regions. Note that the lower-mass sideband, $(M_{J/\psi} - 13\sigma,\ M_{J/\psi} - 10\sigma)$, is further displaced from the nominal J/ψ mass than the upper-mass sideband, $(M_{J/\psi} + 5\sigma,\ M_{J/\psi} + 8\sigma)$, in order to avoid any effects from the radiative tail of the J/ψ mass distribution. The fit to the data uses a double Gaussian for the signal and a linear background shape starting at 2.74 GeV/c^2. The center of the wide Gaussian floats in order to fit the radiative tail on the low-mass side of the J/ψ peak. The wide Gaussian contributes $< 5\%$ of the yield.

The dimuon trigger accepts J/ψ candidates both from prompt production and from B-hadron decays. We suppress the B-hadron contribution by selecting on the sum of squares of the impact parameter significance of the two muon tracks at a level studied with Monte Carlo events. We only accept events satisfying the following requirement:

$$S \equiv \left(\frac{d_0(\mu^+)}{\sigma_{d_0(\mu^+)}}\right)^2 + \left(\frac{d_0(\mu^-)}{\sigma_{d_0(\mu^-)}}\right)^2 \leq 8. \tag{3}$$

This removes most of the long-lived background and gives a final prompt J/ψ sample of 783,600 events above a background of 61,700 events with small contamination from B-hadron decays, to be quantified in Sec. VI. The invariant mass distribution of the final sample is shown in Fig. 1 (a). We divide these events into six $p_T(\mathrm{J}/\psi)$ ranges for the polarization fit. The invariant mass distributions for the six p_T ranges of J/ψ are shown in Fig. 2. Table I shows the dimuon mass fit resolution for each $p_T(\mathrm{J}/\psi)$ bin. The total number of events in the J/ψ signal region, N_D, and the number of sideband background events, N_B, are also given for each bin. The number of signal events, N_S, is estimated by sideband subtraction, $N_D - N_B$. This is the information needed for the polarization analysis.

The same data sample also contains approximately 166,300 J/ψ events from B-hadron decays, as given in Fig. 1 (b). The polarization for these events should be independent of the $p_T(\mathrm{J}/\psi)$. We applied the polarization analysis to these data. The templates developed for the prompt decays apply equally well to the B-decay events, since the change in transverse vertex position is tiny compared to the distance to the COT. The p_T distribution is different from that of prompt J/ψ events and is corrected by reweighting.

We select B-decay events by having:

$$S > 16. \tag{4}$$

The simulation studies show that the residual prompt signal beyond this cut is $\leq 10^{-5}$ of the prompt yield. The invariant mass distributions for the six p_T ranges of J/ψ are shown in Fig. 3. The dimuon mass fit for each $p_T(\mathrm{J}/\psi)$ bin for B-decay candidates is also summarized in Tbl. I.

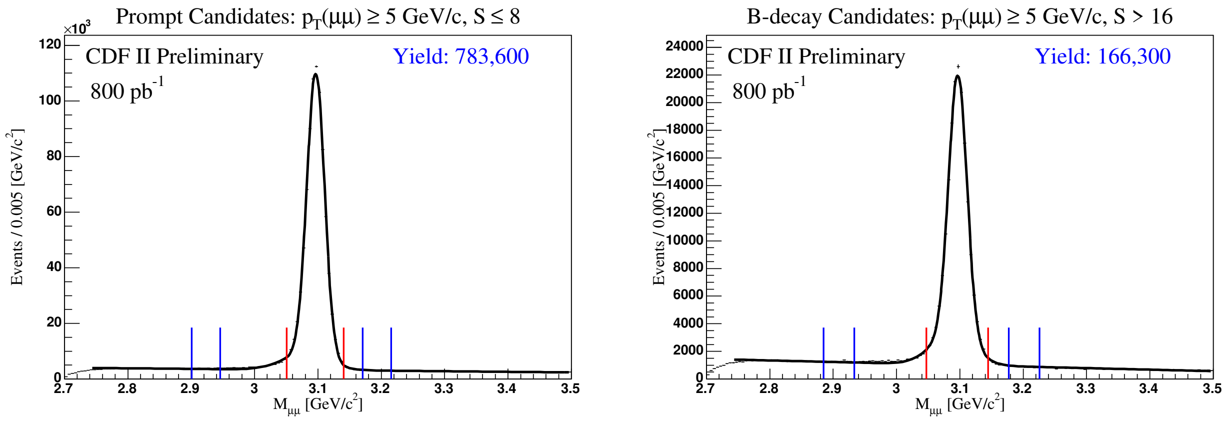

FIG. 1: The invariant mass distribution of the final J/ψ candidate events; (a) J/ψ candidate events selected to measure the prompt J/ψ spin alignment and (b) J/ψ candidate events from B-decays.

IV. ACCEPTANCE & EFFICIENCY

A. Monte Carlo Generation

The CDF realistic simulation software package was used for Monte Carlo (MC) generation. Events were generated by a single particle generator using the acceptance-corrected $p_T(\mathrm{J}/\psi)$ spectrum [8] in the $4 \leq p_T < 30$ GeV/c region. Events were generated uniform in J/ψ rapidity for $|\mathrm{y}| < 1.2$ and in ϕ. The $p_T(\mathrm{J}/\psi)$ cut in analysis is 5 GeV/c. We generated from 4 GeV/c to avoid any systematic bias due to resolution smearing effects. The generated J/ψ was decayed with the QQ decay package. In QQ, we can control the J/ψ polarization. Three different samples were generated: completely unpolarized (U) sample of about 20M events, fully transversely polarized (T) sample of about 190M events, and fully longitudinally polarized (L) sample of about 140M events. After decay, events were processed through the sequence of detector simulation and offline reconstruction. We generate more T events because their acceptance is lower than L events.

$p_T(\mathrm{J}/\psi)$: mean $p_T(\mathrm{J}/\psi)$ [GeV/c]	signal region [MeV/c^2] $[M_{\mathrm{J}/\psi}-3\sigma,\ M_{\mathrm{J}/\psi}+3\sigma)$	σ [MeV/c^2]	sideband #1 [MeV/c^2] $[M_{\mathrm{J}/\psi}-13\sigma,\ M_{\mathrm{J}/\psi}-10\sigma)$	sideband #2 [MeV/c^2] $[M_{\mathrm{J}/\psi}+5\sigma,\ M_{\mathrm{J}/\psi}+8\sigma)$	N_D	N_B	N_S	χ^2/d.o.f
all candidates	3052.28−3139.46	14.53	2906.98−2950.57	3168.52−3212.11	2765248	311292	2453956 ± 1754	584.46
$p_T(\mathrm{J}/\psi) \geq 5$	3050.01−3141.45	15.24	2897.61−2943.33	3171.93−3217.65	1103371	89181	1014190 ± 1092	199.12
$p_T(\mathrm{J}/\psi) \geq 5$, prompt (8)	3050.76−3140.64	14.98	2900.96−2945.90	3170.60−3215.54	845229	61660	783569 ± 952	136.23
5−6 : 5.47	3052.84−3138.82	14.33	2909.54−2952.53	3167.48−3210.47	322414	26523	295891 ± 591	60.68
6−7 : 6.46	3051.20−3140.12	14.82	2903.00−2947.46	3169.76−3214.22	204079	14215	189864 ± 467	32.69
7−9 : 7.83	3049.91−3141.35	15.24	2897.51−2943.23	3171.83−3217.55	200372	12023	188349 ± 461	26.89
9−12 : 10.14	3046.86−3144.06	16.20	2884.86−2933.46	3176.46−3225.06	85988	5409	80579 ± 302	12.64
12−17 : 13.72	3041.25−3149.31	18.01	2861.15−2915.18	3185.33−3239.36	26899	2359	24540 ± 171	5.40
17−30 : 19.98	3030.47−3159.41	21.49	2815.57−2880.04	3202.39−3266.86	5602	912	4690 ± 81	2.17
$p_T(\mathrm{J}/\psi) \geq 5$, B-decay (16)	3047.22−3144.66	16.24	2884.82−2933.54	3177.14−3225.86	187180	20849	166331 ± 456	48.74
5−6 : 5.48	3049.16−3142.82	15.61	2893.06−2939.89	3174.04−3220.87	58640	7951	50689 ± 258	18.84
6−7 : 6.47	3048.17−3143.69	15.92	2888.97−2936.73	3175.53−3223.29	40471	4579	35892 ± 212	11.43
7−9 : 7.86	3046.86−3144.54	16.28	2884.06−2932.90	3177.10−3225.94	46335	4407	41928 ± 225	11.83
9−12 : 10.22	3044.96−3146.78	16.97	2875.26−2926.17	3180.72−3231.63	26567	2384	24183 ± 170	6.56
12−17 : 13.88	3042.50−3150.62	18.02	2862.30−2916.36	3186.66−3240.72	11594	1085	10509 ± 113	3.27
17−30 : 20.33	3028.70−3161.96	22.21	2806.60−2873.23	3206.38−3273.01	3389	361	3028 ± 61	1.70

TABLE I: Summary of dimuon mass fit results. Information on signal and sideband regions, resolution, and yield is shown.

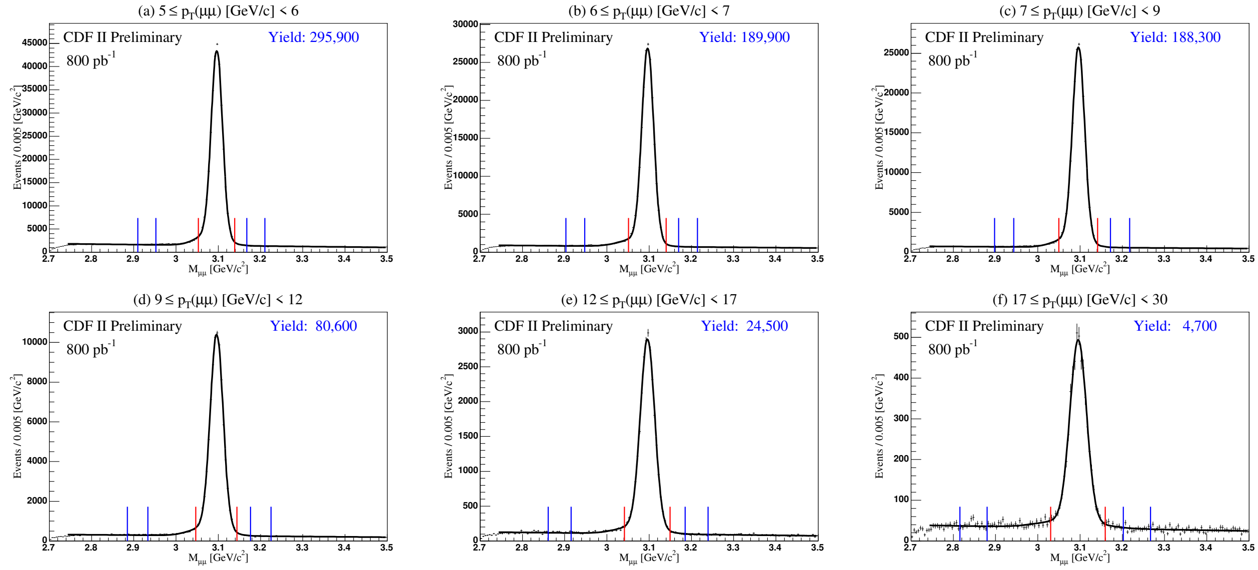

FIG. 2: The invariant mass distributions of the final sample selected to measure the prompt J/ψ spin alignment, separated into six different p_T ranges of J/ψ.

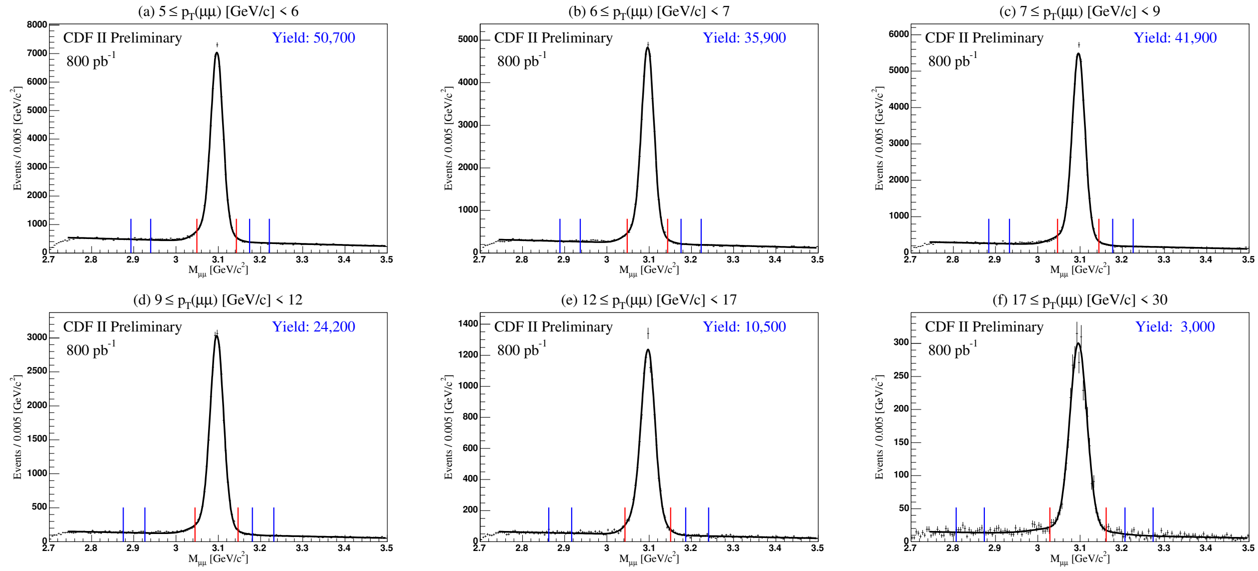

FIG. 3: The invariant mass distributions for the J/ψ candidates from B-decays, separated into six different p_T ranges of J/ψ.

B. Acceptance, Efficiency, and Trigger Effects

The acceptance depends on the polarization. The combined acceptance and trigger effects of the CDF apparatus heavily modify both the J/ψ decay angular distributions and the yields for T and L alignments. This analysis employs a template model that accounts for all the corrections due to acceptance and trigger effects by applying the CDF detector simulation, reconstruction software, and a data-driven trigger efficiency function to the theoretical decay angular distributions before comparing to data in the polarization fitter. We used approximately 150M (100M) events of T (L) type to produce the final templates that will be used in the fit. These events are used only for constructing the templates, so they are statistically independent of all other MC studies to be described in Sec. V. The difference in the total number of generated events between T and L templates are taken into account in the polarization fitter.

After the acceptance and trigger effects are taken into account, the T (L) template sample contains about 3 (3) times the number of events that we have in the data. The distribution in $\cos\theta^*$ for each $p_T(J/\psi)$ region for T and L are shown in Fig. 4. These distributions show the correlation between the p_T cut of muons and acceptance as well as the polarization dependence of the acceptance. One sees that raising the muon p_T threshold reduces the discrimination between T and L polarization. The effect is strongest at low $p_T(J/\psi)$, as expected. The total acceptance for the three different J/ψ polarizations as a function of the $p_T(J/\psi)$ is shown in Table II. The total acceptance includes the geometric and kinematic acceptances, the efficiencies for trigger, and cuts on the event topology.

$p_T(J/\psi)$ [GeV/c]	A_U [%] ($\alpha = 0$)	A_T [%] ($\alpha = +1$)	A_L [%] ($\alpha = -1$)
$5-6$	6.460 ± 0.016	5.208 ± 0.005	8.900 ± 0.008
$6-7$	8.380 ± 0.025	6.926 ± 0.009	11.375 ± 0.013
$7-9$	10.728 ± 0.033	9.024 ± 0.011	14.040 ± 0.016
$9-12$	12.968 ± 0.060	11.241 ± 0.021	16.425 ± 0.030
$12-17$	15.093 ± 0.126	13.632 ± 0.044	18.553 ± 0.062
$17-30$	16.269 ± 0.319	15.077 ± 0.113	18.662 ± 0.151

TABLE II: Total J/ψ acceptance as a function of p_T estimated from three MC samples.

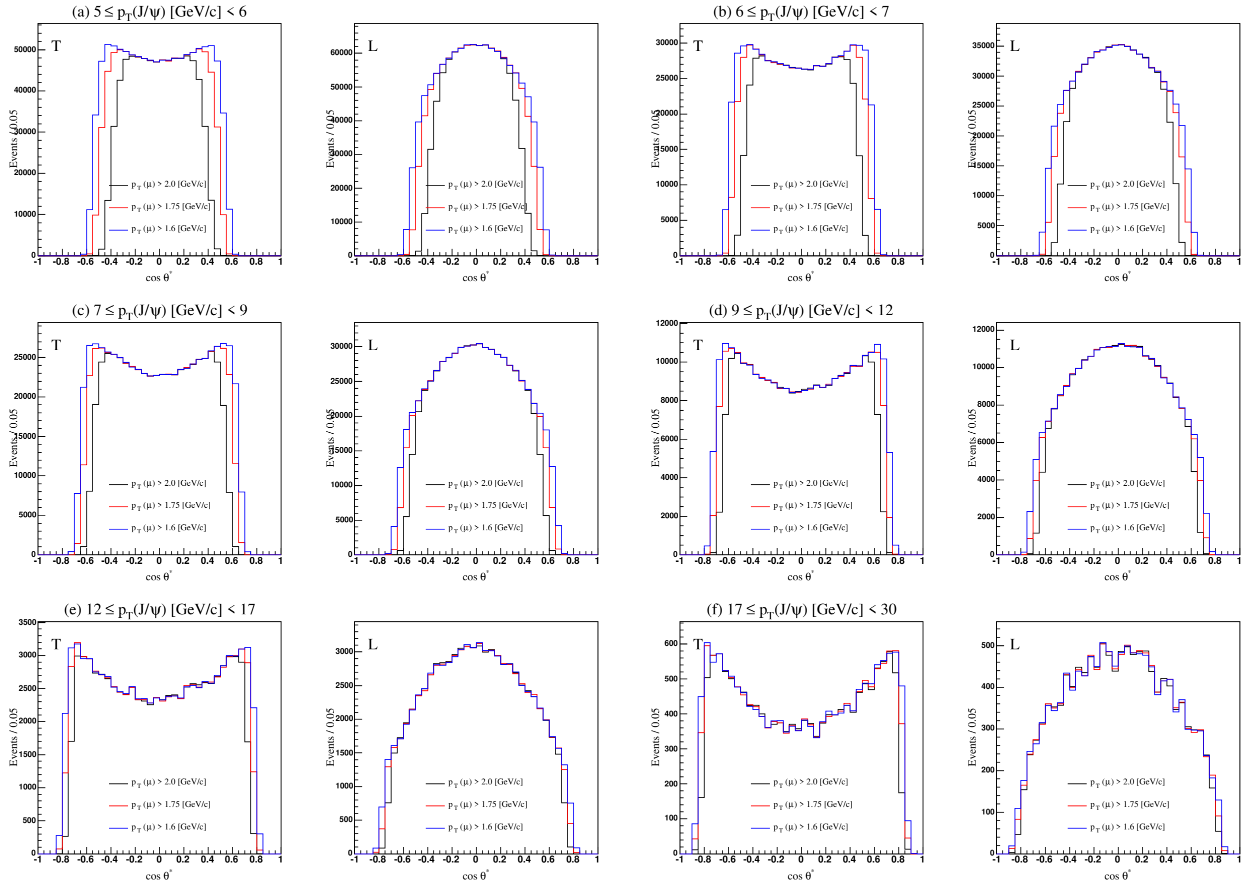

FIG. 4: MC templates are shown for each $p_T(J/\psi)$ bin.

The spin alignment information is contained in the $\cos\theta^*$ distribution for the J/ψ decay. The expected resolution in $\cos\theta^*$ is very good over the entire p_T range according to simulation studies. Based on these results, we have chosen to bin all data in $\cos\theta^*$ bins of 0.05 from -1 to 1. The simulation studies also show that the J/ψ mass distribution is the same for all $\cos\theta^*$ bins for a given p_T range.

V. POLARIZATION FITTER

A. Description of Polarization Fitters

We have implemented a χ^2 fitter. It is a ROOT adaption of the Run I fitter allowing for Poisson-distributed errors. In this fitter, the cos θ^* distribution of the *total*, not sideband-subtracted, events, $D_i(p_T)$, for a given p_T range is binned in 40 equal bins from -1 to 1. The *sideband* events are also binned accordingly, $B_i(p_T)$. The theoretical signal function for cos θ^* bin i is the polarization-weighted sum of the T(p_T) and L(p_T) templates for that bin in this p_T range:

$$ES_i(p_T) = N(\eta; p_T)[(1-\eta) \cdot T_i(p_T) + \eta \cdot L_i(p_T)]. \tag{5}$$

The normalization parameter $N(\eta; p_T)$ matches the total number of events in the mass window for the specific p_T bin to the η-dependent prediction from the templates:

$$N(\eta; p_T) = \frac{\sum_i (D_i(p_T) - B_i(p_T))}{(1-\eta) \cdot \sum_i T_i(p_T) + \eta \cdot \sum_i L_i(p_T)}. \tag{6}$$

The fitter includes an individual background term for each cos θ^* bin, normalized to the total number of sideband events, $\sum_i B_i(p_T)$. The minimization is done simultaneously for the total and sideband distributions.

In order to search for a possible bias in the fitter, we divided the T and L polarization test samples into subsets, then combined the various subsets to make polarization samples with polarization parameters from -1 to $+1$ in steps of 0.2. Each $p_T(\mathrm{J}/\psi)$ bin is represented in these toy studies, but we treated all bins equally, since each bin provided a known input polarization, a fitted polarization, and an error. For each bin analyzed, we calculated the pull p = $(\alpha_{\text{fit}} - \alpha_{\text{input}})/\sigma_{\text{fit}}$. The results for 160 such toy experiments are plotted in Fig. 5.

The fit to the pull distribution in Fig. 5 is a maximum likelihood fit to a Gaussian. The mean is -0.125 ± 0.077 and the Gaussian sigma is 0.970 ± 0.057. Taking the statistical error as $\sqrt{N_{bin}+1}$ for all bins, including the zero bins, the χ^2 of the fit of this pull distribution to a Gaussian is 48.3 for 57 degrees of freedom corresponding to 79% probability. We conclude that there is no statistically-significant indication of any fit bias from these studies. The Run I studies also showed no indication of fit bias for this fitter.

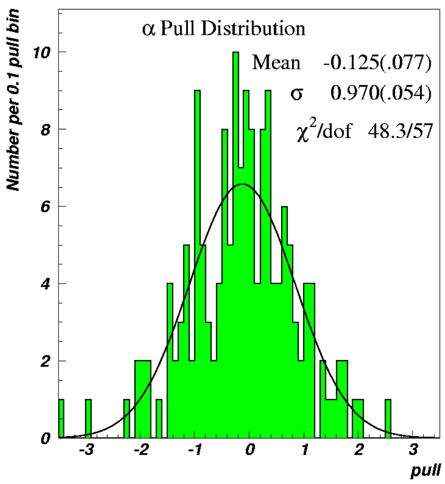

FIG. 5: Pulls from the polarization fits with 160 toy Monte Carlo experiments.

VI. LONG-LIVED BACKGROUND

We have studied the remaining long-lived J/ψ component after making the impact parameter significance cut described in Sec. III. To quantify the residual long-lived contamination B_B after the prompt selection by Eq. 3, we examined the sideband-subtracted proper time (ct) distribution for the J/ψ events in Fig. 6. The figure (a) is the ct distribution before making the prompt selection cut and the figure (b) is the ct distribution after making the cut. In those figures, the negative proper time bins have been reflected about the y-axis (ct = 0) to estimate the prompt Gaussian signal in positive proper time bins. The long-lived excess from heavy-flavor decays is clearly visible before making the cut. After the cut, the long-lived tail is strongly reduced, but not completely.

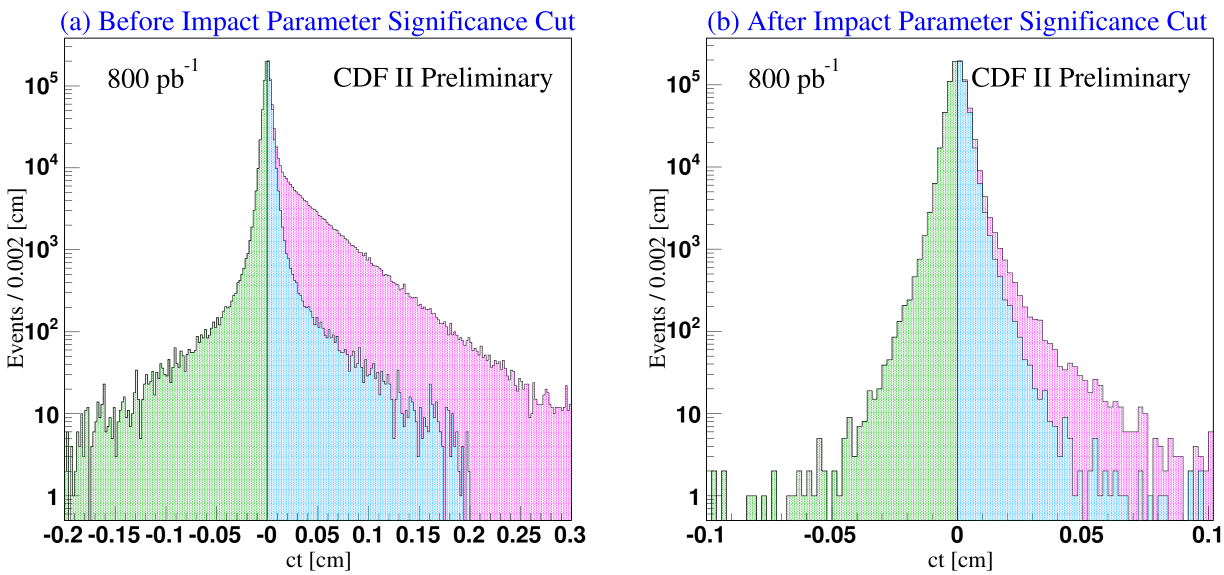

FIG. 6: The sideband-subtracted ct distributions of J/ψ candidate events (a) before and (b) after applying the prompt selection requirement. There are 1,014,200 (783,600) J/ψ candidate events before (after) applying the prompt selection requirement.

We quantify this long-lived background for each $p_T(\mathrm{J}/\psi)$ bin, assuming that the prompt J/ψ signal is a Gaussian distribution centered at ct = 0. The long-lived background is extracted by folding the negative ct distributions about zero and subtracting from the positive ct distributions. The remaining asymmetry in the ct distribution is clear in all $p_T(\mathrm{J}/\psi)$ bins.

We count the number of J/ψ events having negative ct values, N_-, and the number having positive ct values, $N_+ = N_- + N_L$. Subtracting the two quantities gives the amount of long-lived contamination, N_L, with an error given by twice the statistical uncertainty of N_-. Finally, B_B is the percentage ratio of N_L to total, calculated as $N_L/(N_- + N_+)$. The results are shown in Tbl. III. The residual long-lived contamination may be slowly rising with $p_T(\mathrm{J}/\psi)$, but the statistical errors make it hard to tell if there is a change. In any case it is small for all $p_T(\mathrm{J}/\psi)$ bins and is taken into account for the polarization measurement.

The ratio ϵ_{meas}, the number of sideband-subtracted signal events after making the cut over the number of sideband-subtracted signal events before the cut, is the efficiency for the prompt selection requirement estimated from data. The 2$^{\mathrm{nd}}$ column displays the number of events before and after the cut in two rows in each $p_T(\mathrm{J}/\psi)$ bin. The 3$^{\mathrm{rd}}$ column is ϵ_{meas}, as calculated by the 2$^{\mathrm{nd}}$ column. Note that ϵ_{meas} is very different from the efficiency estimated from Monte Carlo ϵ_{MC}, since our Monte Carlo samples consist of only prompt J/ψ signal events.

The non-prompt yield includes mis-measured events, indicated by the negative exponential tail (see Fig. 6 (a)), and B-decays. The overall yield of J/ψ events coming from B-hadron decays, f_B, derived from the numbers in Tbl. III, are consistent with the B-yield as a function of $p_T(\mathrm{J}/\psi)$ measured in Ref. [8]. Refer to the comparison made in Tbl. IV.

VII. RESULTS

For a given $p_T(\mathrm{J}/\psi)$ bin, total and sideband data were separated into $\cos\theta^*$ bins and fit with the fitter described in Sec. V. Polarization fit results for the prompt J/ψ signal in individual p_T bin are shown in Fig. 7. The polarization results are shown in Fig. 8 and tabulated in Tbl. V. The fitted result α_{fit} includes polarization effects from the residual B-decay background. We have unfolded that effect based on the measurements of the B-decay contamination fraction

$p_T(\mathrm{J}/\psi)$ [GeV/c]	$N_{\rm prompt} + N_{B-\rm decay}$ / $N_{\rm prompt}$	$\epsilon_{\rm meas}$ [%]	N_-	N_L	residual B-contamination B_B [%]
≥ 5	1014190 / 783569	77.3	376980	29609	3.8 ± 0.1
$5-6$	369604 / 295891	80.1	143682	8527	2.9 ± 0.2
$6-7$	241103 / 189864	78.7	91705	6454	3.4 ± 0.2
$7-9$	245790 / 188349	76.6	90360	7629	4.1 ± 0.2
$9-12$	111953 / 80579	72.0	37960	4659	5.8 ± 0.3
$12-17$	37442 / 24540	65.5	11448	1644	6.7 ± 0.6
$17-30$	8207 / 4690	57.1	2035	620	13.2 ± 1.4

TABLE III: The summary of study on long-lived background.

mean p_T	5.47	6.46	7.83	10.14	13.72	19.98
$\epsilon_{\rm MC}$	.965	.964	.963	.961	.959	.957
$f_{\rm prompt}$	.806	.789	.763	.706	.637	.518
f_B	.158	.175	.201	.258	.327	.446
f_B (publish)	.15	.185	.20	.26	.33	.49±.05

TABLE IV: The overall yield of J/ψ events coming from B-hadron decays.

B_B in each $p_T(\mathrm{J}/\psi)$ bin given in Tbl. III. The value for the prompt J/ψ polarization $\alpha_{\rm prompt}$ is computed from the fitted result according to the formula:

$$\alpha_{\rm fit} = (1 - B_B) \cdot \alpha_{\rm prompt} + B_B \cdot \alpha_B, \quad \alpha_{\rm prompt} = \frac{\alpha_{\rm fit} - B_B \cdot \alpha_B}{(1 - B_B)}. \tag{7}$$

$p_T(\mathrm{J}/\psi)$ [GeV/c]	N_D	N_S	N_B	Prompt J/ψ polarization		
				$\alpha_{\rm fit}$	$\alpha_{\rm prompt}$	$\chi^2/d.o.f$
$5-6$	322414	295891	26523	$-0.014^{+0.028}_{-0.028}$	$-0.012^{+0.029}_{-0.029} \pm 0.007$	0.84
$6-7$	204079	189864	14215	$-0.012^{+0.027}_{-0.027}$	$-0.010^{+0.028}_{-0.028} \pm 0.007$	1.22
$7-9$	200372	188349	12023	$-0.084^{+0.022}_{-0.021}$	$-0.085^{+0.023}_{-0.022} \pm 0.007$	1.43
$9-12$	85988	80579	5409	$-0.093^{+0.026}_{-0.026}$	$-0.095^{+0.028}_{-0.028} \pm 0.007$	1.12
$12-17$	26899	24540	2359	$-0.137^{+0.040}_{-0.039}$	$-0.142^{+0.043}_{-0.042} \pm 0.007$	1.26
$17-30$	5602	4690	912	$-0.204^{+0.077}_{-0.073}$	$-0.225^{+0.089}_{-0.084} \pm 0.007$	1.01

TABLE V: Prompt J/ψ polarization: The summary of the fit to the data.

CDF measured in Run I that the effective polarization of the J/ψ mesons produced in B-hadron decays $\alpha_B = -0.1 \pm 0.1$ [4]. For $B_{u,d}$ decays there is a precision measurement of $\alpha_B = -0.13 \pm 0.01$ from BaBar studies of inclusive $B \to \mathrm{J}/\psi X$ decays [16]. This was adapted to the hadron collider environment in ref. [8]: $\alpha_B = -0.129 \pm 0.009$. The B-factory result does not include possible polarization effects from B_s and B-baryon decay modes. As will be discussed later we ourselves have measured the polarization of J/ψ mesons from B-hadron decays. Our result is less precise, but it includes effects from heavier B-hadrons than the B-factory results.

The proper time distribution for the J/ψ candidate events from B-decays selected by the requirement (Eq. 4) is shown in Fig. 9. We quantify the residual prompt contamination B_P from the usual method, reflecting the negative-ct bins about the y-axis to estimate the amount of prompt signals in positive ct bins. B_P is the percentage ratio of $2 \cdot N_-$ to total and varies from 23.4% (in the lowest $p_T(\mathrm{J}/\psi)$ bin) to 2.8% (in the highest $p_T(\mathrm{J}/\psi)$ bin). As the data in Fig. 9 shows, the prompt contamination is limited to the region ct ≤ 0.03 cm in all p_T bins. The remaining contamination is from the mis-measured events that populate the exponential tail. We choose to measure the B-decay polarization only for events having ct > 0.03 cm, which reduces the signal by a factor of 2 and contamination by about a factor

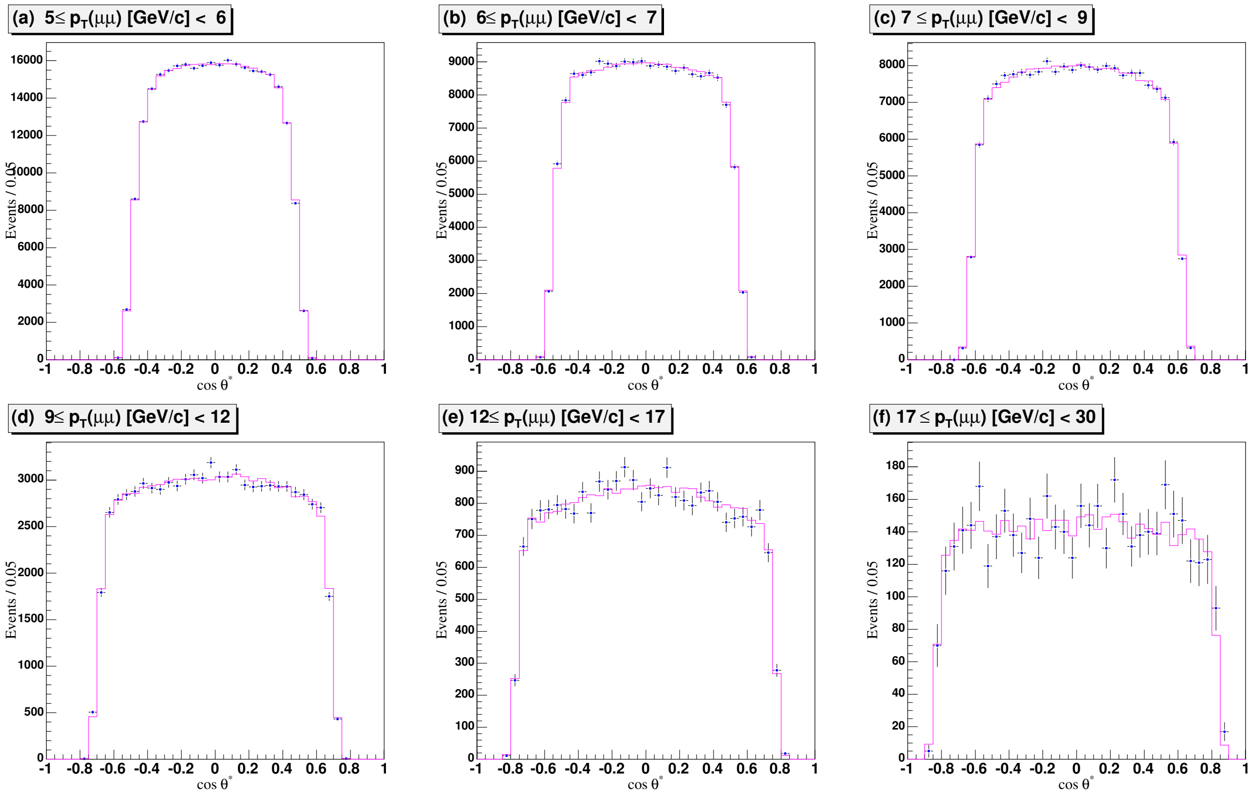

FIG. 7: Polarization fit results for the prompt J/ψ signal.

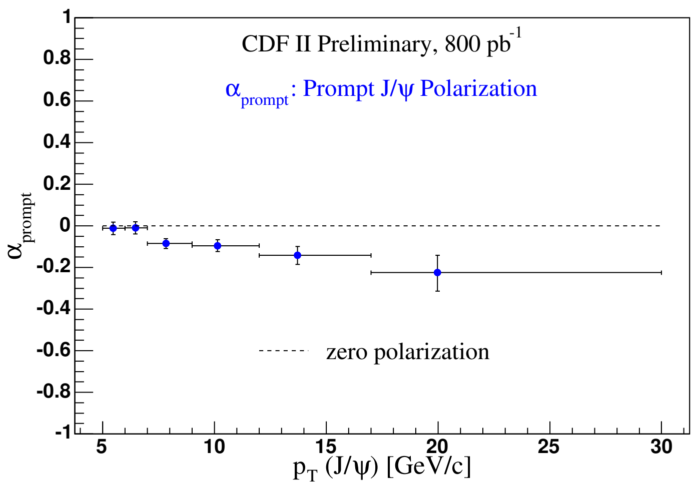

FIG. 8: Prompt J/ψ polarization: Polarization fit results to the data.

of 3−7 according to the $p_T(\mathrm{J}/\psi)$ bin. The remaining contamination ranges from 7.2% to 0.4% after the cut. Because we ascribe the remaining contamination to mismeasured events, we assign zero polarization to the background. The polarization for the B-decay events should be independent of p_T. We correct for contamination bin by bin and then combine all six bins by a χ^2 average. The result is α_B = -0.066 ± 0.050 with χ^2 = 7.6 for 5 degrees of freedom (Prob = 18%). This compares well to the Run I measurement from Ref. [4].

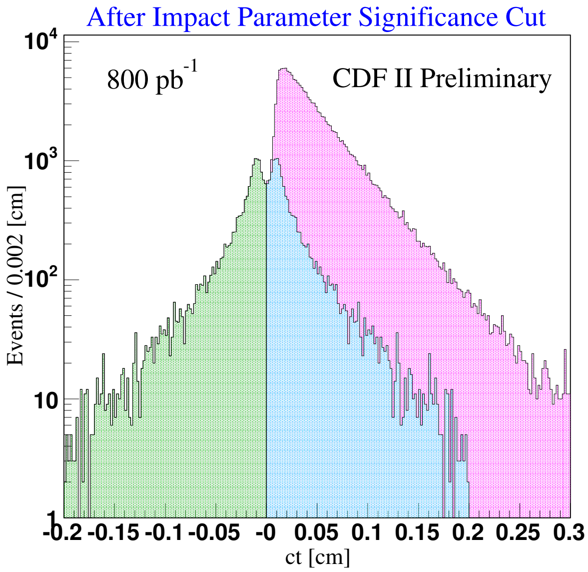

FIG. 9: The sideband-subtracted ct ditribution for the J/ψ candidates from B-decays.

p_T(J/ψ) [GeV/c]	N_D	N_S	N_B	Polarization of J/ψ Mesons from B-decays		
				$\alpha_{\rm fit}$	α_B	$\chi^2/d.o.f$
5 − 6	29501	26648	2853	$+0.212^{+0.102}_{-0.095}$	$+0.228^{+0.110}_{-0.102} \pm 0.032$	1.05
6 − 7	21092	19241	1851	$-0.085^{+0.087}_{-0.082}$	$-0.090^{+0.092}_{-0.087} \pm 0.026$	0.55
7 − 9	25106	23155	1951	$-0.132^{+0.063}_{-0.060}$	$-0.137^{+0.065}_{-0.062} \pm 0.026$	1.07
9 − 12	14732	13579	1153	$-0.042^{+0.067}_{-0.064}$	$-0.043^{+0.069}_{-0.066} \pm 0.026$	0.84
12 − 17	6434	5957	477	$-0.150^{+0.079}_{-0.075}$	$-0.151^{+0.080}_{-0.076} \pm 0.026$	1.13
17 − 30	1835	1678	157	$-0.096^{+0.122}_{-0.113}$	$-0.096^{+0.122}_{-0.113} \pm 0.026$	0.72

TABLE VI: Polarization of J/ψ mesons from B-decays: The summary of the fit to the data.

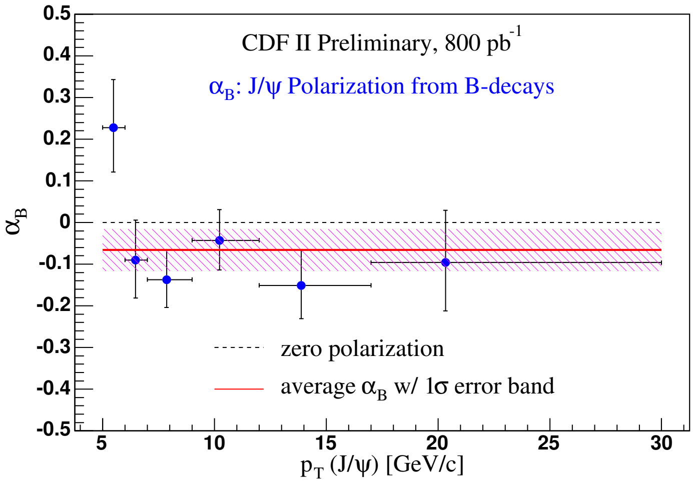

FIG. 10: Polarization of J/ψ mesons from B-decays: Polarization fit results to the data.

VIII. SYSTEMATIC UNCERTAINTIES

The systematic uncertainty on the acceptance is estimated by the change in the polarization parameter α when a modification was made on all trigger efficiencies by $\pm 1\sigma$.

As part of the systematic study, we looked at the polarization for different minimum p_T requirements on the muons. In all cases the p_T threshold of J/ψ remained at 5 GeV/c. There is no systematic change in the prompt polarization as the muon p_T threshold is varied above and below the nominal 1.75 GeV/c cut. However, the B-decay polarization estimate is pulled by the lowest p_T bin, which contributes 5.5 to the total χ^2 sum of 7.6 in Fig. 10. If we exclude that low point, the polarization moves from -0.066 to -0.098. We have no evidence that this point is anything but a statistical fluctuation. Increasing the p_T threshold moves the α value in small steps that are highly correlated. There are no sudden jumps in value. To be conservative we assign this point to have a systematic error of half the difference, or $\Delta\alpha = 0.020$, because of possible dependence on the muon p_T threshold. The results at higher p_T(J/ψ) are coherent and don't move with muon threshold changes. We assign an error $\Delta\alpha = 0.007$ for all higher points.

The remaining systematic errors on the polarization measurement come from systematics in the template generation due to uncertainties in the p_T(J/ψ) spectrum used in the Monte Carlo. The Monte Carlo p_T(J/ψ) spectrum is taken from the Run II data. The measured cross sections in each p_T(J/ψ) bin have only $1-3\%$ errors for p_T(J/ψ) > 5 GeV/c, as used in this analysis. To get a feeling for the effects in this analysis, we note that in the Run I systematics (Tbl. 4.9 in [5]) much larger discrepancies between the data and MC p_T(J/ψ) spectra produced changes in the alignment parameter α of order 0.01. In light of the much smaller errors from the spectral uncertainty, we make an alignment parameter systematic error assignment of 0.002 for the p_T spectrum effects. As another check of possible spectral errors, we compared the mean p_T and the rms p_T spread for the data and the tuned Monte Carlo templates for each of the six p_T(J/ψ) bins. They agree in the third decimal place for each bin. We make no further systematic error allowance for the spectral shape uncertainty.

As described in Sec. VII, the polarization of J/ψ mesons from the decay of B mesons made with light quarks has been measured precisely by the BaBar experiment and translated into an effective $\alpha_B = -0.129 \pm 0.009$ for the kinematics of the Tevatron hadron collider. This polarization parameter does not include polarization shifts due to B_s or b-baryon decay contributions. The new value of α_B reported here matches the Run I central value and is smaller than the BaBar number at the 1.5 σ level. Because we have already assigned a systematic error for possible muon p_T threshold sensitivity that might move the CDF result closer to the BaBar measurement, we assign no further systematic error to the B-decay polarization measurement due to the modest disagreement of the CDF and BaBar numbers, which don't measure exactly the same physical quantity.

We made a separate test of the effect of the long-lived contamination on the prompt polarization by limiting the prompt sample to J/ψ decays having negative proper times. This reduces the long-lived contribution to $< 0.2\%$. For the negative α_B indicated by our B-decay data and the residual B-contamination listed in Tbl. III, removing the B-decay contribution should shift the fitted polarizations by a maximum of -0.01. The changes that we observe are much larger than that, consistent with the increased statistical error. The statistical error for the negative ct selection scales by $\sqrt{2}$, just as one would expect. We conclude that the long-lived B contribution has no observable effect on the fitted prompt polarization.

We changed the $\cos\theta^*$ binning from 0.05 to 0.10. Because the $\cos\theta^*$ resolution shown in Fig. **??** is much smaller than 0.05, we expected no change in the polarization and we saw no change. Therefore, there is no systematic error assigned for the $\cos\theta^*$ binning effect.

The fitter studies with MC show no indication of problems; the fitted polarization agrees well with the value used to generate the input at all p_T.

systematic source	systematic error $\Delta\alpha$	
	(a) prompt polarization	(b) B-decay polarization
acceptance	0.007	0.007
muon p_T cut	0	0.020 (lowest); 0.007 (rest)
global p_T spectrum	0.002	0.024

TABLE VII: Systematic errors in the alignment parameter α for (a) prompt J/ψ events and (b) J/ψ events from B-decays.

IX. CONCLUSIONS

This analysis of the spin alignment of J/ψ mesons produced in the central rapidity region $|y| < 0.6$ shows consistent longitudinal J/ψ alignment over a p_T range of $5-30$ GeV/c. There is a longitudinal alignment at the largest p_T, in contrast to expectations from NRQCD and other models developed to explain the anomalous J/ψ production. This result disagrees with the Run I measurement. Conversely, it matches the prediction of Ref. [7], which stated that the alignment should be longitudinal at least for events with $p_T(\mathrm{J}/\psi) > 15$ GeV/c. Thus, these results open the door to a new theoretical basis for the discussion of the mechanisms for production and polarization of J/ψ mesons in hadronic interactions at high energy.

In order to see the pattern of disagreement with Run I results, we have rebinned the Run II data and templates into the Run I pattern in order to compare better to Run I results. In the reanalysis we raised the muon p_T threshold to 2 GeV/c, the cut used in almost all of Run I data. The two sets of polarization results are shown in Fig. 11. The disagreement comes in the mid-range p_T region for the J/ψ. The Run II acceptances and templates shown in Sec. IV vary smoothly across this p_T range. As seen in Tbl. II the acceptance for the T component of polarization changes almost by a factor of 2 between the bin from $6-7$ GeV/c and the bin from $12-15$ GeV/c. The observed polarization is about the same in the two bins and remains stable as the muon p_T cut is varied from 1.6 to 2 GeV/c.

Both Run I and Run II data tend toward larger longitudinal alignment at $p_T > 15$ GeV/c. This makes it very important for us to pursue the J/ψ polarization with more data and a wider range of muon triggers to extend our reach as far as possible to high p_T. A companion note CDF-8288 outlines similar behavior for ψ' alignment at large p_T. We will also want to look carefully at Υ polarization in order to give further guidance to theory.

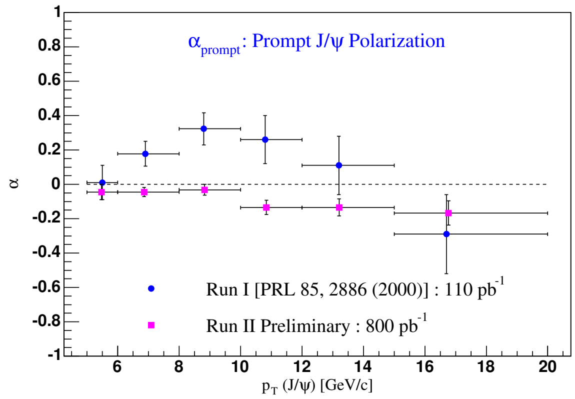

FIG. 11: Run II results reanalyzed in the same $p_T(\mathrm{J}/\psi)$ bins used in Run I and compared to Run I results.

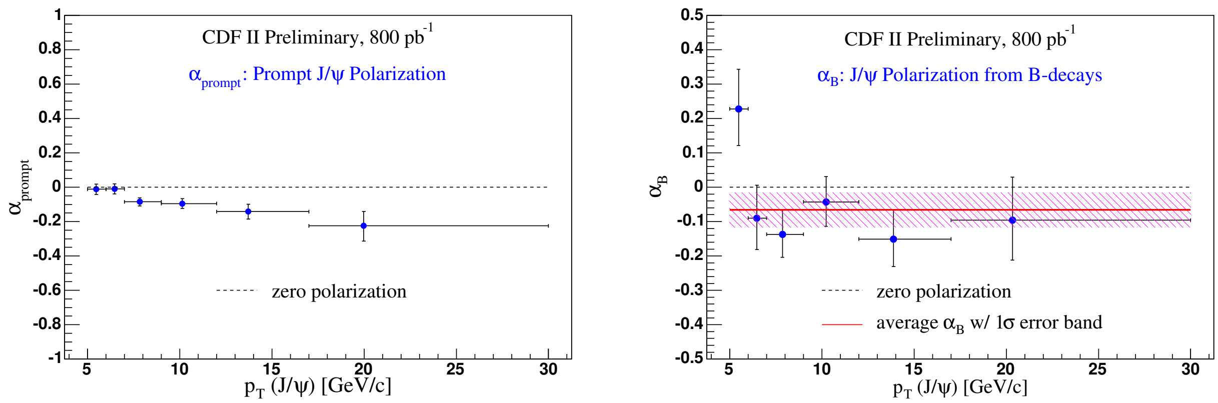

FIG. 12: Run II results on measurement of the prompt and B-decay J/ψ spin alignment in CDF.

Acknowledgments

We thank the Fermilab staff and the technical staffs of the participating institutions for their vital contributions. This work was supported by the U.S. Department of Energy and National Science Foundation; the Italian Istituto Nazionale di Fisica Nucleare; the Ministry of Education, Culture, Sports, Science and Technology of Japan; the Natural Sciences and Engineering Research Council of Canada; the National Science Council of the Republic of China; the Swiss National Science Foundation; the A.P. Sloan Foundation; the Bundesministerium fuer Bildung und Forschung, Germany; the Korean Science and Engineering Foundation and the Korean Research Foundation; the Particle Physics and Astronomy Research Council and the Royal Society, UK; the Russian Foundation for Basic Research; the Comision Interministerial de Ciencia y Tecnologia, Spain; and in part by the European Community's Human Potential Programme under contract HPRN-CT-20002, Probe for New Physics.

[1] CDF Collaboration, F. Abe *et al.*, "J/ψ and $\psi(2S)$ Production in $p\overline{p}$ collisions at $\sqrt{s} = 1.8$ TeV," Phys. Rev. Lett. **79**, 572 (1997).
[2] CDF Collaboration, F. Abe *et al.*, "Production of J/ψ from χ_c decays in $p\overline{p}$ collisions at $\sqrt{s} = 1.8$ TeV," Phys. Rev. Lett. **79**, 578 (1997).
[3] Eric Braaten and Sean Fleming, "Color-Octet Fragmentation and the ψ' Surplus at the Fermilab Tevatron," Phys. Rev. Lett. **74**, 3327 (1995).
[4] CDF Collaboration, T. Affolder *et al.*, "Measurement of J/ψ and $\psi(2S)$ Polarization in $p\overline{p}$ collisions at $\sqrt{s} = 1.8$ TeV," Phys. Rev. Lett. **85**, 2886 (2000).
[5] R.J. Cropp, "A Measurement of the Polarization of J/ψ Mesons Produced in High-Energy $p\overline{p}$ Collisions," CDF Note 5400 (2000).
[6] R. Cropp *et al.*, "A measurement of prompt J/ψ polarization," CDF Note 5029 (1999).
[7] V.A. Khoze, A.D. Martin, M.G. Ryskin, and W.J. Stirling, "Inelastic J/ψ and Υ hadroproduction," Eur. Phys. J. **C 39**, 163−171 (2005).
[8] CDF Collaboration, D. Acosta *et al.*, "Measurement of the J/ψ Meson and b-Hadron Production Cross Sections in $p\overline{p}$ Collisions at $\sqrt{s} = 1960$ GeV," Phys. Rev. D **71**, 032001 (2005).
[9] F. Abe, et al., Nucl. Instrum. Methods Phys. Res. A **271**, 387 (1988); D. Amidei, et al., Nucl. Instum. Methods Phys. Res. A **350**, 73 (1994); F. Abe, et al., Phys. Rev. D **52**, 4784 (1995); P. Azzi, et al., Nucl. Instrum. Methods Phys. Res. A **360**, 137 (1995); The CDFII Detector Technical Design Report, Fermilab-Pub-96/390-E
[10] D. Glenzinski, M. Herndon, T. Kamon, V. Krutelyov, C.-J. Lin, C. Plager, N. Wisniewski, "Measurement of Level-1, 2, and 3 Low-p_T DiMuon Trigger Efficiencies for the $B_s^0 \to \mu^+\mu^-$ Analysis," CDF Note 7314 (2005).
[11] J. Konigsberg *et al.*, "A First Look at the CLC Luminosity Measurements," CDF Note 6052 (2002).
[12] S. Klimenko *et al.*, "Averaging of the inelastic cross-section measured by the CDF and the E811 experiments," CDF Note 6314 (2003).
[13] M. Campanelli *et al.*, "Calibration of the momentum scale for Kalman refitter using J/ψ events," CDF Note 6905 (2004).
[14] M.J. Kim *et al.*, "A Measurement of the Prompt J/ψ Spin Alignment in CDF Run II Data," CDF Note 7484 (2005).
[15] D. Acosta, V. Necula, P. Pfeiffer, M. Schmitt, A. Sukhanov, D. Tsybychev, S.M. Wang "Introduction to Run II Jet Probability Heavy Flavor Tagger," CDF Note 6315 (2003).
[16] B. Aubert *et al.*, "Study of inclusive production of charmonium mesons in B decay," Phys. Rev. D **67**, 032002 (2003), hep-ex/0207097.